International Journal of Engineering, Mathematical and Physical Sciences
ISSN: 2517-9934
Vol:2, No:7, 2008

Flow acoustics in solid-fluid structures

Morten Willatzen and Mikhail Vladimirovich Deryabin

Abstract**—**The governing two-dimensional equations of a heterogeneous material composed of a fluid (allowed to flow in the absence of acoustic excitations) and a crystalline piezoelectric cubic solid stacked one-dimensionally (along the z direction) are derived and special emphasis is given to the discussion of acoustic group velocity for the structure as a function of the wavenumber component perpendicular to the stacking direction (being the x axis). Variations in physical parameters with y are neglected assuming infinite material homogeneity along the y direction and the flow velocity is assumed to be directed along the x direction. In the first part of the paper, the governing set of differential equations are derived as well as the imposed boundary conditions. Solutions are provided using Hamilton's equations for the wavenumber vs. frequency as a function of the number and thickness of solid layers and fluid layers in cases with and without flow (also the case of a position-dependent flow in the fluid layer is considered). In the first part of the paper, emphasis is given to the small-frequency case. Boundary conditions at the bottom and top parts of the full structure are left unspecified in the general solution but examples are provided for the case where these are subject to rigid-wall conditions (Neumann boundary conditions in the acoustic pressure). In the second part of the paper, emphasis is given to the general case of larger frequencies and wavenumber-frequency bandstructure formation. A wavenumber condition for an arbitrary set of consecutive solid and fluid layers, involving four propagating waves in each solid region, is obtained again using the monodromy matrix method. Case examples are finally discussed.

Keywords**—**Flow, acoustics, solid-fluid structures, periodicity.

I. Introduction

IN previous papers on acoustic propagation in periodic composition of fluid layers [1], [2], [3], [5], [4], [6], [7], [8], the phenomena of obtaining effective reduction in the group velocity (below the individual material sound speeds) are discussed and implications for sound-beam focusing, acoustic surgery, and flow measurement presented [9], [10], [11], [6]. In recent works by the authors, results for wavenumber-frequency relations in a finite set of alternating layers of two fluid materials allowing for fluid flows are presented along with discussions of acoustic stability properties. Using the monodromy matrix method analytical results can be obtained for the effective group velocity even in the presence of a fluid flow. In the present work, we extend the analysis to include the practically more relevant case with a finite set of alternating layers of solid and fluid layers (with a possible flow in the fluid layer). The thickness of each solid and fluid layer can be arbitrary as well as the flow-velocity dependence on position in the fluid layer. The solid materials are assumed to be cubic piezoelectric crystals including the simpler case of isotropic solids. Firstly, the general set of governing differential equations, interface, and boundary conditions is derived for the case of small frequencies. A single equation describing the dependence of the group velocity on the number and thicknesss of structure consisting of N solid layers and M fluid layers as well as the flow velocity is obtained. It is shown that a cut-off thickness of the fluid layer relative to the solid layer thickness exists for a set of complete solid and fluid layers $N = M$ below which evanescent waves corresponding to imaginary group velocities are solutions and above which usual travelling waves can propagate. Near this cut-off thickness, changes in the group velocity with flow velocity are significantly amplified if the (tangential) flow velocity at the interface between the fluid and solid layers is nonzero.

In the second part of the paper, discussions are extended to account for the case of larger frequencies. Based on a monodromy matrix method, a wavenumber relation is obtained for a set of N solid layers and M fluid layers. In particular, it is shown that four waves can generally propagate in the solid layer. A case study for wavenumber-frequency bandstructure formation is discussed.

Morten Willatzen and Mikhail Vladimirovich deryabin are with the Mads Clausen Institute for Product Innovation, University of Southern Denmark, DK-6400 Sønderborg, Denmark; email: {willatzen,mikhail}@mci.sdu.dk

II. Theory

In this section, a derivation of the governing differential equations for a structure composed of layers of a solid and a fluid is presented. Interface conditions are derived in the presence of a fluid flow along with boundary conditions imposed. A Hamiltonian method is used to obtain an equation for the group velocity at small frequencies for a structure with a finite number and varying thicknesss of solid and (moving) fluid layers. In the second part, the derivation is extended to account for general frequencies and solid-fluid in alternatingly stacked structures by use of the monodromy matrix method.

A. Solid layer

In the following, we consider a system composed of two materials A and B, where A is a solid layer and B is a fluid layer. The fluid layer is allowed to move, albeit at constant velocity in time, i.e., steady-state flow, in the absence of sound excitation. We do not, unless explicitly stated, assume that the full structure is composed by alternatingly stacking material layers A and B (i.e., local periodicity is not necessary). In the Cartesian coordinate system (x, y, z), we take z as the direction of material inhomogeneity, see Figure 1. Furthermore, we assume monofrequency acoustic excitation, i.e., all dynamic variables vary as $\exp(i\omega t)$ with ω the frequency and t is time.

The Navier's equations representing the acoustic equations for the solid A read:

$$\frac{\partial T_{ij}}{\partial x_j} = -\rho_A \omega^2 u_i, \qquad i = 1, 2, 3, \tag{1}$$

with T_{ij}, x_j, ρ_A, and u_i the stress tensor, the spatial coordinates $[(x_1, x_2, x_3) = (x, y, z)]$, the mass density of material

A, and the displacement components, respectively. Repeated indices are to be summed over (Einstein notation). The stress tensor relates to the strain tensor S_{ij} according to Hooke's law in addition to piezoelectric effects accounting for the crystalline nature of material A. In other words:

$$T_{ij} = c_{ijkl}S_{kl} - e_{ijk}E_k, \quad (2)$$

$$S_{ij} = \frac{1}{2}\left(\frac{\partial u_i}{\partial x_j} + \frac{\partial u_j}{\partial x_i}\right), \quad (3)$$

where c_{ijkl} is the stiffness tensor components allowed by crystal symmetry, e_{ijk} is the piezoelectric e tensor, and E_k is the k'th component of the electric field. Finally, we must include the Poisson equation:

$$\frac{\partial D_i}{\partial x_i} = \rho_{free}, \quad (4)$$

where D_i is the electric displacement and ρ_{free} is the free-carrier charge density supplemented by the constitutive relation:

$$D_i = \epsilon_{ij}E_j + e_{ijk}S_{jk}, \quad (5)$$

with ϵ_{ij} the permittivity tensor.

In order to simplify the above system, we will analyze cases where the material-system dimensions in the x and y directions are much larger than along the z direction. This allows for considering the well-known (infinite-plate) capacitor conditions, i.e., the electric field and the electric displacement point along the z direction:

$$E_1 = E_2 = 0, \quad (6)$$

$$D_1 = D_2 = 0. \quad (7)$$

Considering also that no free electrical charges are present in the system, Equation (4) simplifies to:

$$\frac{\partial D_3}{\partial z} = 0. \quad (8)$$

Employing the constitutive relation [Equation (5)] then gives:

$$\frac{\partial E_3}{\partial z} = -\frac{e_{3jk}}{\epsilon_{33}}\frac{\partial S_{jk}}{\partial z}. \quad (9)$$

If, as is usually the case, the fluid is an insulator, electric currents cannot move through the system. At ultrasonic frequencies the important contribution to the electric current is the displacement current being proportional to the electric displacement. Thus, we may simplify further and require

$$D_3 = 0, \quad (10)$$

which by use of Equation (5) allows for augmenting the electric field in terms of the strain coefficients:

$$E_3 = -\frac{e_{3jk}}{\epsilon_{33}}S_{jk}. \quad (11)$$

Employing Equations (11), (2) in Equation (1) yields

$$\left(c_{ijkl} + \frac{e_{ij3}e_{3kl}}{\epsilon_{33}}\right)\frac{\partial S_{kl}}{\partial x_j} = -\rho_A\omega^2 u_i, \quad (12)$$

which upon combining with the strain definition in terms of (elastic) displacements are three second-order differential equations in the (elastic) displacements. Notice that the effect of piezoelectricity is simply to alter the effective stiffness from c_{ijkl} to $c_{ijkl} + \frac{e_{ij3}e_{3kl}}{\epsilon_{33}}$.

In order to obtain specific equations, information about the crystal symmetry of material A is necessary. Consider material A to be a zinc-blende crystal (cubic, piezoelectric crystal due to lack of inversion symmetry). We have also assumed that our variables do not depend on y. The three Navier equations [Equation (12)] become:

$$c_{11}\frac{\partial^2 u_1}{\partial x^2} + c_{12}\frac{\partial^2 u_3}{\partial x \partial z} + \frac{c_{44}}{2}\frac{\partial}{\partial z}\left(\frac{\partial u_1}{\partial z} + \frac{\partial u_3}{\partial x}\right) = -\rho_A\omega^2 u_1, \quad (13)$$

$$\left(\frac{c_{44}}{2} + \frac{e_{x4}^2}{2\epsilon_{33}}\right)\left(\frac{\partial^2 u_2}{\partial x^2} + \frac{\partial^2 u_2}{\partial z^2}\right) = -\rho_A\omega^2 u_2, \quad (14)$$

$$c_{11}\frac{\partial^2 u_3}{\partial z^2} + c_{12}\frac{\partial^2 u_1}{\partial x \partial z} + \frac{c_{44}}{2}\frac{\partial}{\partial x}\left(\frac{\partial u_1}{\partial z} + \frac{\partial u_3}{\partial x}\right) = -\rho_A\omega^2 u_3, \quad (15)$$

following the contracted tensor notation used in, e.g., Ref. [12]. If material A is an isotropic solid, the above equations simplify to

$$c_{11}\frac{\partial^2 u_1}{\partial x^2} + c_{12}\frac{\partial^2 u_3}{\partial x \partial z} + \frac{c_{11}-c_{12}}{4}\frac{\partial}{\partial z}\left(\frac{\partial u_1}{\partial z} + \frac{\partial u_3}{\partial x}\right) = -\rho_A\omega^2 u_1, \quad (16)$$

$$\frac{c_{11}-c_{12}}{4}\left(\frac{\partial^2 u_2}{\partial x^2} + \frac{\partial^2 u_2}{\partial z^2}\right) = -\rho_A\omega^2 u_2, \quad (17)$$

$$c_{11}\frac{\partial^2 u_3}{\partial z^2} + c_{12}\frac{\partial^2 u_1}{\partial x \partial z} + \frac{c_{11}-c_{12}}{4}\frac{\partial}{\partial x}\left(\frac{\partial u_1}{\partial z} + \frac{\partial u_3}{\partial x}\right) = -\rho_A\omega^2 u_3, \quad (18)$$

since piezoelectric coefficients are zero and $c_{44} = (c_{11} - c_{12})/2$ in the case of isotropic solids. Note that the form of the above system of differential equations is the same for zinc-blende and isotropic crystals.

Observe that the approximations made lead to decoupling of u_2 from the u_1, u_3 (elastic) displacement components in the case with zinc-blende crystal symmetry (and of course also for isotropic crystals). The above equations can be further simplified due to the material homogeneity along the x direction. This fact allows us to search for solutions in the form:

$$\frac{\partial u_i}{\partial x} = i\beta u_i. \quad (19)$$

Parameter β will be referred to as a *wavenumber*.

Observe that the approximations made lead to decoupling of u_2 from the u_1, u_3 (elastic) displacement components in the case with zincblende crystal symmetry (and of course also for isotropic crystals). The above equations can be further simplified due to the material homogeneity along the x direction. This fact allows us to search for solutions in the form:

$$\frac{\partial u_i}{\partial x} = i\beta u_i. \quad (20)$$

Parameter β will be referred to as a *wavenumber*.

Insertion of Equation (20) in Equation (13)-(15) leads to (for zincblende crystals):

$$-\beta^2 c_{11}u_1 + i\beta c_{12}\frac{\partial u_3}{\partial z} + \frac{c_{44}}{2}\frac{\partial}{\partial z}\left(\frac{\partial u_1}{\partial z} + i\beta u_3\right) = -\rho_A\omega^2 u_1, \quad (21)$$

$$-\beta^2\left(\frac{c_{44}}{2} + \frac{e_{x4}^2}{2\epsilon_{33}}\right)u_2 + \frac{\partial^2 u_2}{\partial z^2} = -\rho_A\omega^2 u_2, \quad (22)$$

$$c_{11}\frac{\partial^2 u_3}{\partial z^2} + i\beta c_{12}\frac{\partial u_1}{\partial z} + \frac{c_{44}}{2}i\beta\left(\frac{\partial u_1}{\partial z} + i\beta u_3\right) = -\rho_A\omega^2 u_3, \quad (23)$$

while for isotropic solids:

$$-\beta^2 c_{11}u_1 + i\beta c_{12}\frac{\partial u_3}{\partial z} + \frac{c_{11}-c_{12}}{4}\frac{\partial}{\partial z}\left(\frac{\partial u_1}{\partial z} + i\beta u_3\right) = -\rho_A\omega^2 u_1, \quad (24)$$

$$-\beta^2\frac{c_{11}-c_{12}}{4}u_2 + \frac{\partial^2 u_2}{\partial z^2} = -\rho_A\omega^2 u_2, \quad (25)$$

$$c_{11}\frac{\partial^2 u_3}{\partial z^2} + i\beta c_{12}\frac{\partial u_1}{\partial z} + \frac{c_{11}-c_{12}}{4}i\beta\left(\frac{\partial u_1}{\partial z} + i\beta u_3\right) = -\rho_A\omega^2 u_3. \quad (26)$$

Remark. This is in fact a real-valued system of equations: to see it, one has to denote $iu_1 = w_1$, i.e., to consider real-valued u_3 and imaginary u_1. This choice of notation is natural, and we shall see that when we couple two layers together: for purely imaginary u_1, the pressure p in layer B is a real-valued function (cf. relation (46) below).

B. Fluid layer

For the fluid layer B, the governing non-viscous equations read:

$$\frac{\partial \rho_B}{\partial t} + \frac{\partial(\rho_B v_j)}{\partial x_j} = 0, \quad (27)$$

$$\frac{\partial v_i}{\partial t} + v_j\frac{\partial v_i}{\partial x_j} = -\frac{1}{\rho_B}\frac{\partial p}{\partial x_i}, \quad (28)$$

where v_i is the i'th component of the fluid particle velocity, ρ_B is the mass density of material B, and p is the fluid pressure.

We assume that the background flow is stationary, with the velocity

$$\mathbf{v}_0 = (v_0, 0, 0), \quad p = p_0, \quad \rho = \rho_0, \quad (29)$$

We linearize Equations (28) in the neighbourhood of the stationary flow (29), making use of the following assumption: $p_0 = const$ (while the background velocity v_0 needs not to be constant). From now on, we *replace* $\mathbf{v}, p$ and ρ_B by $\mathbf{v} + \mathbf{v}_0, p + p_0$ and $\rho + \rho_0$ respectively, and *consider the parameters* $\mathbf{v}, p$ *and* ρ *being small acoustic perturbations.*

Using the isentropic condition

$$p = c^2\rho, \quad (30)$$

and the monofrequency condition:

$$\frac{\partial}{\partial t} = i\omega,$$

the linearized equations for the acoustic flow become

$$\begin{aligned}
\frac{i\omega}{c^2}p + \frac{v_0}{c^2}\frac{\partial p}{\partial x} + \rho_0\Big(\frac{\partial v_1}{\partial x} + \frac{\partial v_2}{\partial y} + \frac{\partial v_3}{\partial z}\Big) &= 0,\\
i\omega v_1 + v_0\frac{\partial v_1}{\partial x} + v_2\frac{\partial v_0}{\partial y} + v_3\frac{\partial v_0}{\partial z} &= -\frac{1}{\rho_0}\frac{\partial p}{\partial x},\\
i\omega v_2 + v_0\frac{\partial v_2}{\partial x} &= -\frac{1}{\rho_0}\frac{\partial p}{\partial y},\\
i\omega v_3 + v_0\frac{\partial v_3}{\partial x} &= -\frac{1}{\rho_0}\frac{\partial p}{\partial z},
\end{aligned} \quad (31)$$

see Ref. [8] for details.

Next, we are looking for solutions in the B-layer in the same monofrequent form as above for the layer A (keeping the assumption that there is no y-dependence):

$$\frac{\partial p}{\partial x} = i\beta p, \quad \frac{\partial \mathbf{v}}{\partial x} = i\beta\mathbf{v}. \quad (32)$$

As above, we assume that the functions ρ_0 and v_0 do not depend on y, and we assume that the pressure p does not depend on y either. Substituting relations (32) into equations (31), we get the following expression for the pressure p, cf. Ref. [8]:

$$\frac{\partial}{\partial z}\Big(\frac{1}{\rho_0(\omega+\beta v_0)^2}\frac{\partial p}{\partial z}\Big) + \Big(\frac{1}{c^2\rho_0} - \frac{\beta^2}{\rho_0(\omega+\beta v_0)^2}\Big)p = 0. \quad (33)$$

C. Coupling

The above set equations in layer A and B constitutes the full differential-equation framework. In order to complete the model, we need to describe the interface and boundary conditions. Notice that, in the layer A we have (actually) two second-order equations for u_1 and u_3, while in the layer B we have one second-order equation for the pressure p. To solve the whole system, we have to know the relations between u_1, u_3 and p and their derivatives at the $A-B$ boundary.

At interfaces between materials A and B we require that the shear stresses are zero (since material B is considered an ideal, non-viscous fluid and stresses are continuous everywhere through the full structure). We also impose continuity of the normal stresses (pressure), i.e.,

$$T_{13} = T_{23} = 0, \quad \text{at } A-B \text{ interfaces}, \quad (34)$$

$$T_{33} = p, \quad \text{at } A-B \text{ interfaces}. \quad (35)$$

Finally, we impose continuity of normal particle velocity at $A-B$ interfaces:

$$i\omega u_3 = v_3, \quad \text{at } A-B \text{ interfaces}. \quad (36)$$

For the full-structure end-point boundary conditions [at $z = z_L$ and $z = z_R$], we will consider:

$$p_{input} = T_{33}(z = z_L), \quad (37)$$

$$T_{13}(z = z_L) = T_{23}(z = z_L) = 0, \quad (38)$$

$$u_3(z = z_R) = 0, \quad (39)$$

$$T_{13}(z = z_R) = T_{23}(z = z_R) = 0, \quad (40)$$

where p_{input} is assumed to be a known input pressure acting on the structure at $z = z_L$, while the other end of the structure [at $z = z_R$] is rigid. Both ends are not subject to shear stresses.

Expressions for the stress components T_{13}, T_{23}, T_{33} in terms of displacements are needed when imposing the boundary conditions listed in Equations (34)-(40):

$$T_{13} = \frac{c_{44}}{2}\left(\frac{\partial u_1}{\partial z} + \frac{\partial u_3}{\partial x}\right), \quad (41)$$

$$T_{23} = \frac{c_{44}}{2}\frac{\partial u_2}{\partial z}, \quad (42)$$

$$T_{33} = c_{12}\frac{\partial u_1}{\partial x} + c_{11}\frac{\partial u_3}{\partial z}. \quad (43)$$

We notice also that ϵ_{33} for a cubic crystal (and for isotropic crystals) equals ϵ_{11}.

Due to Equation (31), we get

$$(i\omega + i\beta v_0)v_z = -\frac{1}{\rho_0}\frac{\partial p}{\partial z}. \quad (44)$$

As $v_z = i\omega u_3$ (the continuity of the normal velocity at the $A-B$ interface), we get:

$$i\omega(i\omega + i\beta v_0)u_3 = -\frac{1}{\rho_0}\frac{\partial p}{\partial z}. \quad (45)$$

Applying relation $T_{33} = p$ on the interface, we get:

$$c_{12}i\beta u_1 + c_{11}\frac{\partial u_3}{\partial z} = p. \quad (46)$$

As $T_{13} = 0$ on the interface, we have:

$$\frac{\partial u_1}{\partial z} + i\beta u_3 = 0. \quad (47)$$

Conditions (45)-(47) are enough to solve completely our system. Indeed, let p and $\partial p/\partial z$ be given at the beginning of a layer A, i.e., if this layer is given by relation $z \in [z_L^A, z_R^A]$, then p and its derivative are given at $z = z_L^A$. In order to find the pressure and its derivative at $z = z_R^A$, we solve system (21)-(23) [or (24)-(26)] subject to the boundary conditions above. At $z = z_L^A$, conditions (45)-(47) must be satisfied while Equation (47) applies at $z = z_R^A$. Thus, four boundary conditions are given which uniquely define the solution of system (21)-(23). Next, at $z = z_R^A$, we use relations (45, 47)so as to determine p and $\partial p/\partial z$. Notice that the mapping

$$p, \partial p/\partial z\,|_{z=z_L^A} \to p, \partial p/\partial z\,|_{z=z_R^A}$$

is linear, and one can find the monodromy matrix for this system. We then solve Equation (33) with these initial conditions at $z = z_R^A$, and so on. Thus, the above set of equations is solved following a procedure similar to the one presented in Refs. [7], [8].

Remark. Notice that formally, we have systems of different dimensions in layers A and B: A four-dimensional system in A (two second-order differential equations) and a two-dimensional system in B (two first-order differential equations). The complete system is however well-defined by the conditions at the boundaries between layers A and B as mentioned above.

III. Group velocity

The group velocity for our composite media is defined by

$$c_g = \frac{\partial\omega}{\partial\beta}|, \quad (48)$$

see Ref. [6]. In this section, we only consider the group velocity in the case where ω tends to zero as β tends to zero.

To determine the function $\omega(\beta)$, one has to solve the whole system with the boundary conditions at $z = z_L$ and $z = z_R$.

We first rewrite Equation (33) in the following form. We introduce the variable

$$q = \frac{1}{\rho_0(\omega + \beta v_0)^2}\frac{\partial p}{\partial z}. \quad (49)$$

Equation (33) now becomes

$$q' = -\frac{\partial H}{\partial p}, \quad p' = \frac{\partial H}{\partial q}, \quad (50)$$

which are Hamilton's equations, where $(\cdot)' = \partial/\partial z$, and the Hamiltonian equals

$$H(p,q) = \frac{1}{2}\Big(\rho_0(\omega + \beta v_0)^2 q^2 + \Big(\frac{1}{c^2\rho_0} - \frac{\beta^2}{\rho_0(\omega + \beta v_0)^2}\Big)p^2\Big). \quad (51)$$

To find the derivative $\partial\omega/\partial\beta$, the following trick is used. We substitute $\omega = c_g\beta + O(\beta^2)$ into the full system of equations, tend $\beta \to 0$, and then write down the solution to these equations – instead of first solving the equations, and then tending $\beta \to 0$. This is a correct operation, as the equations depend regularly on β: the right-hand side of Equations (50) tends to a finite limit as $\beta \to 0$, $\omega \to 0$, $\omega/\beta \to c_g$, and so do Equations (21)-(23) [or (24)-(26)] and the boundary conditions (45).(47). Thus, by Poincaré's theorem, on any bounded interval, the solution to Hamilton's equations for $\beta \to 0$, $\omega \to 0$, $\omega/\beta \to c_g$ tends to the solution at $\beta = 0$, $\omega = 0$, $\omega/\beta = c_g$. Notice that in this limit case, the group velocity coincides with the phase velocity $c_p = \omega/\beta$.

Remark. Observe that, as $\beta, \omega \to 0$, Equation (33) becomes singular. This has apparently been the reason for numerical inaccuracies in solving Equation (33) in Ref. [6]. As we have shown, the singularity is removed by passing to Hamiltonian equations.

In the A layer, we get from Equations (21)-(23) the following system of equations as $\omega, \beta \to 0$

$$\frac{\partial^2 u_1}{\partial z^2} = 0, \quad \frac{\partial^2 u_3}{\partial z^2} = 0. \quad (52)$$

In the B layer, we have from Equation (49)-(50)

$$p' = 0, \quad q' = -\frac{1}{\rho_0}\left(\frac{1}{c_B^2} - \frac{1}{(c_g + v_0)^2}\right)p. \quad (53)$$

The boundary conditions are:

$$\frac{\partial u_1}{\partial z} = 0, \quad u_3 = \left(1 + \frac{v_0}{c_g}\right)q, \quad c_{11}\frac{\partial u_3}{\partial z} = p. \quad (54)$$

System (52, 53, 54) can be readily solved. Let the n-th $A-B$ layer start at $z = z_A^n$ and end at $z = z_A^{n+1}$ (the n-th sub-layer A is given by $z \in [z_A^n, z_B^n]$, and the n-th sub-layer B is given by $z \in [z_B^n, z_A^{n+1}]$). We also assume that the background velocity v_0 may depend on z, however, the values of the velocity on the interfaces of $A-B$-layers $v_0(z_A^n), v_0(z_A^n)$ are all the same and equal $v_{A,B}$ (for example, a natural assumption could be $v_{A,B} = 0$).

The pressure p equals the same constant in each B layer: $p = p_0$, while the transformation of q after the passage through one $A-B$ layer is given by

$$q_{n+1} = q_n - \frac{p_0}{\rho_0}\int_{z_B^n}^{z_A^{n+1}}\left(\frac{1}{c_B^2} - \frac{1}{(c_g + v_0)^2}\right)dz + \frac{p_0}{c_{11}(1 + v_{A,B}/c_g)}(z_B^n - z_A^n). \quad (55)$$

Relation (55) allows the value of the group velocity c_g to be found. Suppose that the whole domain consists of N A layers and M B layers of thickness L_A^i $(i = 1, 2, ..., N)$ and L_B^j $(j = 1, 2, ..., M)$, respectively (clearly, $|M - N| \le 1$),

and that q should be zero when $z = z_L$ and $z = z_R$ (rigid embedding walls). Then, from Equation (55) we get:

$$\sum_{i=1}^{N} \frac{L_A^i}{c_{11}(1+v_{A,B}/c_g)} - \frac{1}{\rho_0} \sum_{j=1}^{M} \int_{z_B^j}^{z_A^{j+1}} \left(\frac{1}{c_B^2} - \frac{1}{(c_g+v_0)^2} \right) dz = 0, \quad (56)$$

where $L_A^i = z_B^i - z_A^i$ and $L_B^j = z_A^{j+1} - z_B^j$. The above expression is remarkably simple and general. It applies readily for an arbitrary number of layers and arbitrary individual layer thickness.

If $v_0 = const = v_{A,B}$, then (56) is a quadratic equation for c_g, and the solution can be easily found explicitly. First, we rewrite Equation (56) in the following form:

$$c_g(c_g+v_0) \sum_{i=1}^{N} \frac{L_A^i}{c_{11}} - \frac{1}{\rho_0} \left(\frac{(c_g+v_0)^2}{c_B^2} - 1 \right) \sum_{j=1}^{M} L_B^j = 0, \quad (57)$$

(here we have assumed that $c_g \neq -v_0$). The solution to Equation (57) is given by:

$$c_g = \frac{-\Lambda_2 \pm \sqrt{\Lambda_2^2 - \Lambda_1 \Lambda_3}}{\Lambda_1}, \quad (58)$$

provided $\Lambda_1 \neq 0$, where we have denoted

$$\Lambda_1 = \sum_{i=1}^{N} \frac{L_A^i}{c_{11}} - \frac{1}{\rho_0 c_B^2} \sum_{j=1}^{M} L_B^j,$$
$$2\Lambda_2 = v_0 \sum_{i=1}^{N} \frac{L_A^i}{c_{11}} - \frac{2v_0}{\rho_0 c_B^2} \sum_{j=1}^{M} L_B^j,$$
$$\Lambda_3 = \frac{1}{\rho_0} \sum_{j=1}^{M} L_B^j. \quad (59)$$

One can readily see that, with v_0 being fixed, the group velocity is *a function of the ratio* $\sum_{i=1}^{N} L_A^i / \sum_{j=1}^{M} L_B^j$ *only*, and does not depend on the number or precise distribution of layers.

Expression (56) simplifies for $M = N$ (provided all layers are identical):

$$\frac{L_A}{c_{11}(1+v_{A,B}/c_g)} - \frac{1}{\rho_0} \int_0^{L_B} \left(\frac{1}{c_B^2} - \frac{1}{(c_g+v_0)^2} \right) dz = 0. \quad (60)$$

When the layers are identical, except for some fixed number of layers (for example, the first one and the last one are not complete, or there is some local irregularity in the middle of the structure), Equation (57) provides the asymptotics of the group velocity when the number of layers N tends to infinity for *arbitrary bounded boundary conditions*. Indeed, let the "pressure gradient" q be bounded on both sides of the domain, and let N be the number of $A-B$ layers. Then, the increase of q should be of order $1/N$ over each $A-B$-layer.

Remark. Strictly speaking, we have only shown that the equation for the group velocity for a finite number of layers tends to a similar equation for infinite number of layers. In principle, the solutions may behave differently. For example, we must be careful whenever Equation (59) has degenerate solutions. For example, in the case with $\Lambda_1 = 0$, only one solution exists for c_g but the number of distinct group velocities is not one as the number of layers approaches infinity.

IV. Dispersion relations

As noted above, the system of Equations (23), (50), and (51) with boundary conditions (45-(47) can be solved explicitly. We may use the monodromy matrix (for the mapping of p and q across an $A-B$ block) to find all possible (ω, β) solutions, i.e., not only those for which $\beta, \omega \to 0$ for the case with alternatingly stacked A and B layers.

To find the monodromy matrix, we only need to find the mapping over the A-layer, which we assume to the the isotropic solid. The governing equations are:

$$\frac{c_{11}-c_{12}}{4} \frac{\partial^2 w_1}{\partial z^2} + (\rho_A \omega^2 - c_{11}\beta^2) w_1 - \left(\beta c_{12} + \beta \frac{c_{11}-c_{12}}{4} \right) \frac{\partial u_3}{\partial z} = 0,$$
$$c_{11} \frac{\partial^2 u_3}{\partial z^2} + \left(\rho_A \omega^2 - \frac{c_{11}-c_{12}}{4} \beta^2 \right) u_3 + \left(\beta c_{12} + \beta \frac{c_{11}-c_{12}}{4} \right) \frac{\partial w_1}{\partial z} = 0. \quad (61)$$

Integration of this system (known in classical mechanics, as a system with gyroscopic forces) is performed in the standard way, see, e.g., [13]. First, we make the following notations: we omit indices of w and u, denote by $' = \partial/\partial z$, and denote

$$A_1 = \frac{c_{11}-c_{12}}{4}, \quad B_1 = \rho_A \omega^2 - c_{11}\beta^2,$$
$$C = \beta c_{12} + \beta \frac{c_{11}-c_{12}}{4},$$
$$A_2 = c_{11}, \quad B_2 = \rho_A \omega^2 - \frac{c_{11}-c_{12}}{4} \beta^2. \quad (62)$$

Equations (61) become

$$A_1 w'' + B_1 w - C u' = 0, \quad A_2 u'' + B_2 u + C w' = 0. \quad (63)$$

The eigenvalues λ_i, $i = 1-4$, satisfy the condition

$$\det \begin{pmatrix} A_1\lambda^2 + B_1 & -C\lambda \\ C\lambda & A_2\lambda^2 + B_2 \end{pmatrix} = 0. \quad (64)$$

This gives a bi-quadratic equation

$$(A_1\lambda^2 + B_1)(A_2\lambda^2 + B_2) + C^2\lambda^2 = 0, \quad (65)$$

which has solutions

$$\lambda^2 = \frac{-(A_1B_2 + A_2B_1 + C^2)}{2A_1A_2} \pm \frac{\sqrt{(A_1B_2 + A_2B_1 + C^2)^2 - 4A_1A_2B_1B_2}}{2A_1A_2}. \quad (66)$$

The eigenvectors that correspond to these eigenvalues are given by

$$\xi_i = (A_2\lambda_i^2 + B_2, -C\lambda_i), \quad i = 1, \ldots, 4, \quad (67)$$

and the general solution is:

$$w = \sum_{i=1}^{4} c_i (A_2\lambda_i^2 + B_2) e^{\lambda_i z}, \quad u = -\sum_{i=1}^{4} c_i C \lambda_i e^{\lambda_i z}, \quad (68)$$

where c_i are constants, determined by the initial conditions.

In our case, at all boundaries/interfaces the condition $T_{13} = 0$ applies. Hence,

$$w' - \beta u = 0. \tag{69}$$

Substituting this condition in the solution gives:

$$\sum_{i=1}^{4} \left(c_i \lambda_i (A_2 \lambda_i^2 + B_2) + \beta c_i C \lambda_i \right) = 0,$$

$$\sum_{i=1}^{4} \left(c_i \lambda_i (A_2 \lambda_i^2 + B_2) e^{\lambda_i L_A} + \beta c_i C \lambda_i e^{\lambda_i L_A} \right) = 0, \tag{70}$$

where $L_A = z_B^n - z_A^n$, see Section III. Here we have assumed that the width of each A-layer is the same (otherwise, just replace L_A by L_A^n everywhere below).

In case of $\lambda_1 \neq \lambda_2 \pmod{2\pi i / L_A}$, one can express c_1 and c_2 through c_3 and c_4 by use of Equations (70):

$$c_1 = \frac{\sum_{i=3}^{4} c_i \left(A_2 \lambda_i^2 + B_2 + \beta C \lambda_i \right) \left(e^{\lambda_i L_A} - e^{\lambda_2 L_A} \right)}{\left(A_2 \lambda_1^2 + B_2 + \beta C \lambda_1 \right) \left(e^{\lambda_1 L_A} - e^{\lambda_2 L_A} \right)}$$

$$c_2 = \frac{\sum_{i=3}^{4} c_i \left(A_2 \lambda_i^2 + B_2 + \beta C \lambda_i \right) \left(e^{\lambda_i L_A} - e^{\lambda_1 L_A} \right)}{\left(A_2 \lambda_2^2 + B_2 + \beta C \lambda_2 \right) \left(e^{\lambda_2 L_A} - e^{\lambda_1 L_A} \right)}. \tag{71}$$

The solution can now be written in the following matrix form:

$$\begin{pmatrix} w(z) \\ u(z) \end{pmatrix} = \alpha(z) \begin{pmatrix} c_3 \\ c_4 \end{pmatrix}, \tag{72}$$

where the matrix $\alpha(z)$ has the components

$$\alpha_{11} = \sum_{i=1}^{2} \frac{\left(A_2 \lambda_3^2 + B_2 + \beta C \lambda_3 \right) \left(e^{\lambda_3 L_A} - e^{\lambda_{3-i} L_A} \right)}{\left(A_2 \lambda_i^2 + B_2 + \beta C \lambda_i \right) \left(e^{\lambda_i L_A} - e^{\lambda_{3-i} L_A} \right)} (A_2 \lambda_i^2 + B_2) e^{\lambda_i z} + (A_2 \lambda_3^2 + B_2) e^{\lambda_3 z},$$

$$\alpha_{12} = \sum_{i=1}^{2} \frac{\left(A_2 \lambda_4^2 + B_2 + \beta C \lambda_4 \right) \left(e^{\lambda_4 L_A} - e^{\lambda_{3-i} L_A} \right)}{\left(A_2 \lambda_i^2 + B_2 + \beta C \lambda_i \right) \left(e^{\lambda_i L_A} - e^{\lambda_{3-i} L_A} \right)} (A_2 \lambda_i^2 + B_2) e^{\lambda_i z} + (A_2 \lambda_4^2 + B_2) e^{\lambda_4 z},$$

$$\alpha_{21} = -\sum_{i=1}^{2} \frac{\left(A_2 \lambda_3^2 + B_2 + \beta C \lambda_3 \right) \left(e^{\lambda_3 L_A} - e^{\lambda_{3-i} L_A} \right)}{\left(A_2 \lambda_i^2 + B_2 + \beta C \lambda_i \right) \left(e^{\lambda_i L_A} - e^{\lambda_{3-i} L_A} \right)} C \lambda_i e^{\lambda_i z} - C \lambda_3 e^{\lambda_3 z},$$

$$\alpha_{22} = -\sum_{i=1}^{2} \frac{\left(A_2 \lambda_4^2 + B_2 + \beta C \lambda_4 \right) \left(e^{\lambda_4 L_A} - e^{\lambda_{3-i} L_A} \right)}{\left(A_2 \lambda_i^2 + B_2 + \beta C \lambda_i \right) \left(e^{\lambda_i L_A} - e^{\lambda_{3-i} L_A} \right)} C \lambda_i e^{\lambda_i z} - C \lambda_4 e^{\lambda_4 z}. \tag{73}$$

We can now find an expression for the pressure p and pressure gradient q after passing a single A-layer. To get this expression, we employ the boundary conditions at the $A-B$-layer:

$$p = i\beta c_{12} u_1 + c_{11} \frac{\partial u_3}{\partial z}, \quad q = \frac{\omega}{\omega + \beta v_0} u_3. \tag{74}$$

If we introduce the matrices

$$\mu = \begin{pmatrix} c_{12}\beta & 0 \\ 0 & \frac{\omega}{\omega + \beta v_0} \end{pmatrix}, \quad \nu = \begin{pmatrix} 0 & c_{11} \\ 0 & 0 \end{pmatrix}, \tag{75}$$

the following expressions apply:

$$\begin{pmatrix} p(z_A^n) \\ q(z_A^n) \end{pmatrix} = \left(\mu \alpha(z_A^n) + \nu \alpha'(z_A^n) \right) \begin{pmatrix} c_3 \\ c_4 \end{pmatrix}, \tag{76}$$

$$\begin{pmatrix} w(z_B^n) \\ u(z_B^n) \end{pmatrix} = \alpha(z_B^n) \left(\mu \alpha(z_A^n) + \nu \alpha'(z_A^n) \right)^{-1} \begin{pmatrix} p(z_A^n) \\ q(z_A^n) \end{pmatrix}, \tag{77}$$

and finally,

$$\begin{pmatrix} p(z_B^n) \\ q(z_B^n) \end{pmatrix} = \left(\left(\mu \alpha(z_B^n) + \nu \alpha'(z_B^n) \right) \left(\mu \alpha(z_A^n) + \nu \alpha'(z_A^n) \right)^{-1} \right) \begin{pmatrix} p(z_A^n) \\ q(z_A^n) \end{pmatrix}, \tag{78}$$

Example. Consider the simplest case, when the material consists of a solid A-layer. Let the boundary conditions be $q = 0$. To determine the wavenumber β from a given ω, one must solve the following equation for β:

$$\begin{pmatrix} 0 & 1 \end{pmatrix} \left(\left(\mu \alpha(z_B^n) + \nu \alpha'(z_B^n) \right) \left(\mu \alpha(z_A^n) + \nu \alpha'(z_A^n) \right)^{-1} \right) \begin{pmatrix} 1 \\ 0 \end{pmatrix} = 0. \tag{79}$$

The matrix

$$M_{A_n} = \left(\mu \alpha(z_B^n) + \nu \alpha'(z_B^n) \right) \left(\mu \alpha(z_A^n) + \nu \alpha'(z_A^n) \right)^{-1}, \tag{80}$$

is the monodromy matrix for our system corresponding to the n'th A-layer. In the B-layer, the equation system for p, q is a linear first-order Hamiltonian system, and finding the monodromy matrix M_{B_n} for the mapping of p, q over the n'th B-layer is given in Ref. [8]:

$$M_{B_n} = \begin{pmatrix} \cos \sqrt{F_1 F_2} \left(z_A^{n+1} - z_B^n \right) & \sqrt{\frac{F_1}{F_2}} \sin \sqrt{F_1 F_2} \left(z_A^{n+1} - z_B^n \right) \\ -\sqrt{\frac{F_2}{F_1}} \sin \sqrt{F_1 F_2} \left(z_A^{n+1} - z_B^n \right) & \cos \sqrt{F_1 F_2} \left(z_A^{n+1} - z_B^n \right) \end{pmatrix}, \tag{81}$$

with

$$F_1 = \rho_0 (\omega + \beta v_0)^2, \quad F_2 = \frac{1}{c_B^2 \rho_0} - \frac{\beta^2}{\rho_0 (\omega + \beta v_0)^2}. \tag{82}$$

Thus, the monodromy matrix for p, q for the complete n-th $A-B$-layer is $M_n = M_{B_n} \cdot M_{A_n}$ (layer A comes first).

The equation for the wavenumber β under conditions $q = 0$ on z_L, z_R is (cf. Example above)

$$\begin{pmatrix} 0 & 1 \end{pmatrix} M_R \cdot M_N \cdot M_{N-1} \cdot \ldots \cdot M_1 \cdot M_L \begin{pmatrix} 1 \\ 0 \end{pmatrix} = 0, \tag{83}$$

where N is the number of complete $A-B$ layers, and matrices M_L and M_R are the monodromy matrices for mappings from the initial point z_L to the starting point z_A^1 of the first complete $A-B$-layer, and from the ending point z_A^{N+1} of the last complete $A-B$-layer to the end-point z_R of the structure.

V. Numerical results and discussions

Consider first the case with small β, ω values corresponding to the first part of the Theory section. The group velocity in the absence of a fluid flow for a complete number N of layers A and B becomes using Equation (60):

$$c_g = \frac{c_B}{\sqrt{1 - \frac{c_B^2 \rho_0}{c_{11}} \frac{L_A}{L_B}}}, \tag{84}$$

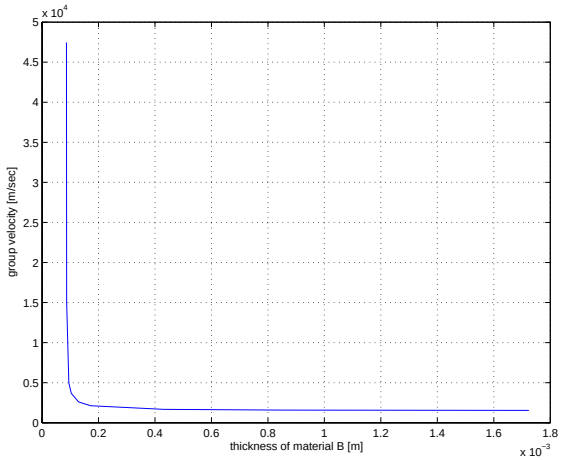

Fig. 1. Variation of the group velocity (at zero flow velocity) with the thickness of the fluid layer for a structure with N complete layers of material A (stainless steel - isotropic solid) and B (water) [i.e., $N = M$]. The thickness of the solid layer: L_A is fixed to be 0.01 m.

thus, we have infinite group velocity if

$$L_B = L_A \frac{c_B^2 \rho_0}{c_{11}} \equiv L_B^{thres}. \quad (85)$$

In other words, when $L > L_B^{thres}$, all wavenumber solutions are imaginary corresponding to evanescent wave propagation. When $L < L_B^{thres}$, propagation along the x direction (perpendicular to the stacking direction) is sinusoidal.

In Figure 1, we show the variation of the group velocity (at zero flow velocity) with the thickness of the fluid layer for a structure with N complete layers of material A (stainless steel - isotropic solid) and B (water) [i.e., $N = M$]. The thickness of the solid layer: L_A is fixed to be 0.01 m. Evidently, as Equation (84) reveals, the group velocity is a function of the ratio L_A/L_B only [refer to the discussion before Equation (60)] and it diverges when $L_B = L_B^{thres}$. For a steel-water structure, the threshold water-layer thickness is: $L_B^{thres} = 0.013 L_A$. Other material data used in the computations in this section are: $c_{11} = 2.61 \cdot 10^{11}$ Pa, $c_{12} = 1.06 \cdot 10^{11}$ Pa, $\rho_A = 7500$ kg/m^3, $c_B = 1500$ m/sec, and $\rho_0 = 1000$ kg/m^3.

Figure 2 (upper plot) shows the continuous variation of the absolute value of the group velocity as a function of the full structure thickness at zero flow. Again, we consider a structure composed of alternating layers of stainless steel and water. The lower plot displays the total material A (dash-dotted) and material B (dashed) thickness parts of the full structure as a function of the full structure thickness (solid). Parameters used are $L_A = 0.01$ m and $L_B = 2.5 L_B^{thres}$ for each complete A and B layer in the full structure. The last layer is generally an incomplete layer of material A type if the secondlast complete layer is of material B type and vice versa. More interesting, note that when the structure thickness equals $L_A + L_B^{thres} = 0.0101$ m or an integer number of $L_A + L_B^{thres}$, the group velocity becomes infinite. However, the structure thickness never equals $N\left(L_A + L_B^{thres}\right)$ for $N > 1$ since a complete B layer thickness equals $2.5 L_B^{thres}$. Furthermore, for thicknesses below $L_A + L_B^{thres}$, the group velocity is imaginary

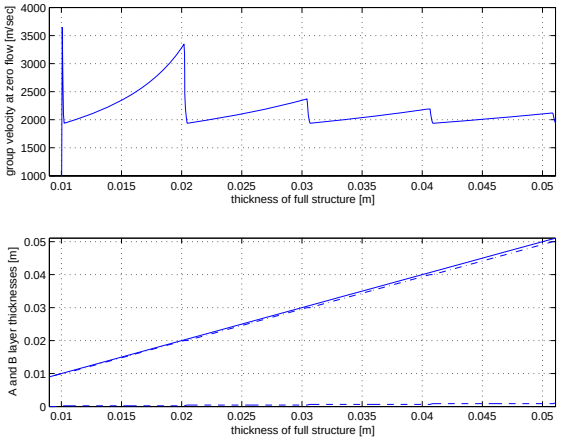

Fig. 2. The upper plot shows the continuous variation of the absolute value of the group velocity as a function of the full structure thickness at zero flow. The structure is composed of alternating layers of stainless steel and water. The lower plot displays the total material A (dash-dotted) and material B (dashed) thickness parts of the full structure as a function of the full structure thickness (solid). Parameters used are $L_A = 0.01$ m and $L_B = 2.5 L_B^{thres}$ for each complete A and B layer in the full structure.

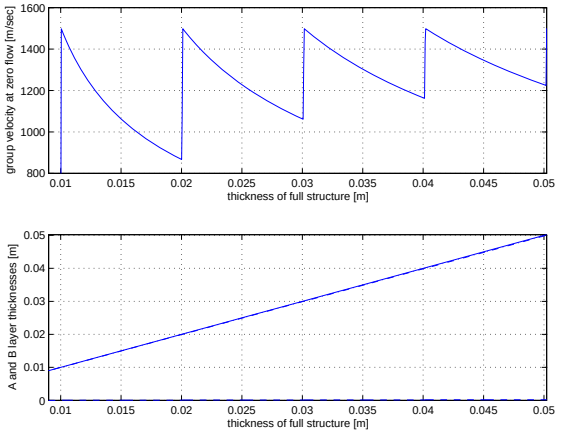

Fig. 3. Continuous variation of the absolute value of the group velocity as a function of the full structure thickness at zero flow for parameter values: $L_A = 0.01$ m and $L_B = 0.5 L_B^{thres}$ for each complete A and B layer in the full structure. Otherwise, conditions are the same as described in the text for Figure 2.

corresponding to evanescent modes. Observe also the step behavior in the absolute value of the group velocity as the full structure thickness increases. This is understandable keeping in mind the large differences in the stiffness values of stainless steel and water ($c_{11} = 2.61 \cdot 10^{11}$ Pa vs. $\rho_0 c_B^2 = 2.25 \cdot 10^9$ Pa).

Figure 3 shows the continuous variation of the absolute value of the group velocity as a function of the full structure thickness at zero flow for parameter values: $L_A = 0.01$ m and $L_B = 0.5 L_B^{thres}$. Otherwise, conditions are the same as described in the text for Figure 2. Note that the distance between steps in structure thickness is smaller than for the case with $L_B = 10 L_B^{thres}$ since the thickness of a complete unit block of material A and B is smaller than above. In

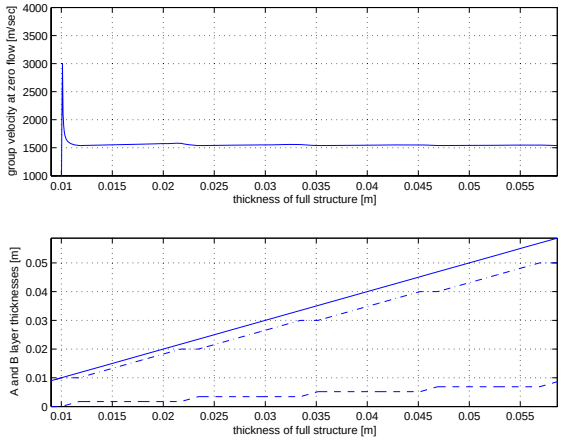

Fig. 4. Computed results are shown for $L_B = 20L_B^{thres}$ otherwise the conditions described for Figure 2 apply.

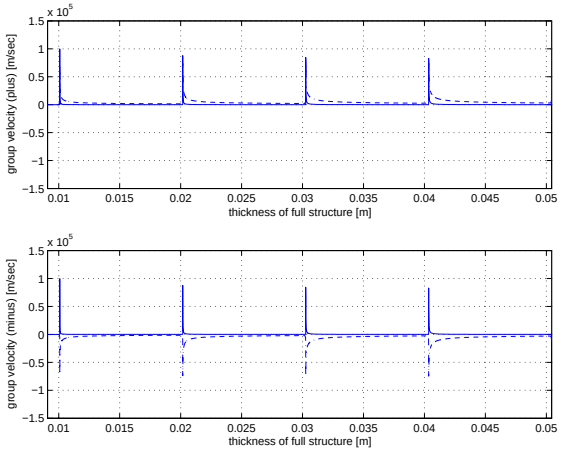

Fig. 5. Continuous variation of the (positive) and (negative) group velocity solutions to Equation (58) as a function of total structure thickness. The fluid flow velocity equals approximately 30 m/sec such that only one group velocity solution (albeit doubly degenerate) exists when the structure thickness equals a complete layer of material A and B. Refer to further details in the textual description.

this case, where the thickness of the structure never equals $N(L_A + L_B^{thres})$ with N an integer, an infinite group velocity is not possible.

In Figure 4, computed results are shown for $L_B = 20L_B^{thres}$ otherwise the conditions described for the two preceding Figures apply.

In Figure 5, the two group velocities computed from Equation (58) are plotted as a continuous function of the total structure thickness. The upper plot shows the real (solid) and imaginary (dashdotted) components of the group velocity corresponding to choosing the positive sign in front of the square root in Equation (58) (denoted the positive solution). Similarly, the lower plot shows the real (solid) and imaginary (dashdotted) components of the group velocity corresponding to choosing the negative sign in front of the square root in Equation (58) (denoted the negative solution). The fluid flow

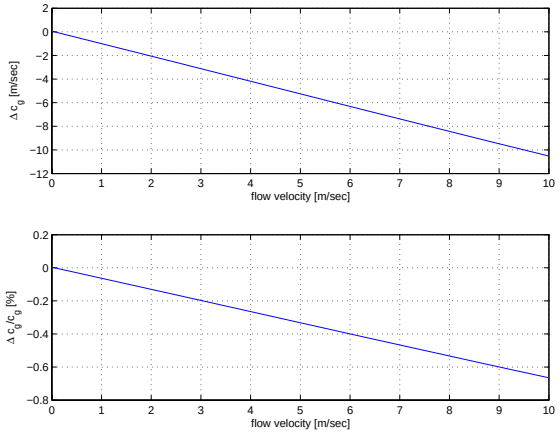

Fig. 6. The upper plot shows the change in group velocity as a function of fluid flow velocity for a structure with $L_B = 10L_B^{thres}$ (same number of complete layers, the starting and ending layers are both complete layers).

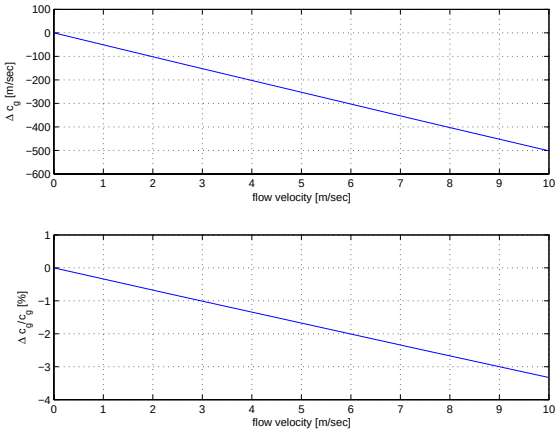

Fig. 7. The upper plot shows the change in group velocity as a function of fluid flow velocity for a structure with $L_B = 1.01L_B^{thres}$. Otherwise same conditions as in Figure 6.

velocity v_0 is chosen to be such that the square root vanishes when the total structure thickness is one complete block of material A and B. In this case, a complete B layer has a thickness equal to $L_B = 0.9999L_B^{thres}$ for which v_0 equals approximately 30 m/sec. Observe that the peaks located near integer values of 0.01 m correspond to places for which the two group velocities are the same (degeneracy). Such a case (with nonzero group velocities) occurs only if $v_0 \neq 0$ as one easily verifies from Equation (58).

In Figure 6, we show (upper plot) the change in group velocity as a function of fluid flow velocity for a structure with $L_B = 10L_B^{thres}$. Observe that the group velocity changes exactly by the fluid flow velocity. In the lower plot, the relative change in group velocity due to the fluid flow is shown.

In Figure 7, we show (upper plot) the change in group velocity as a function of fluid flow velocity for a structure with $L_B = 1.01L_B^{thres}$. Note that the flow-induced group-velocity change is pronouncedly higher than the flow velocity

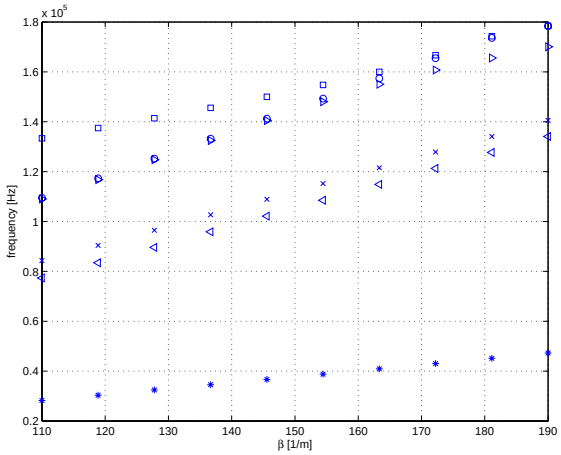

Fig. 8. Plot of the first bands (in frequency) in the β interval: $110-180$ m^{-1} for a structure composed of an A layer (steel) with thickness 0.01 m and a B-layer(water) with thickness 0.001 m.

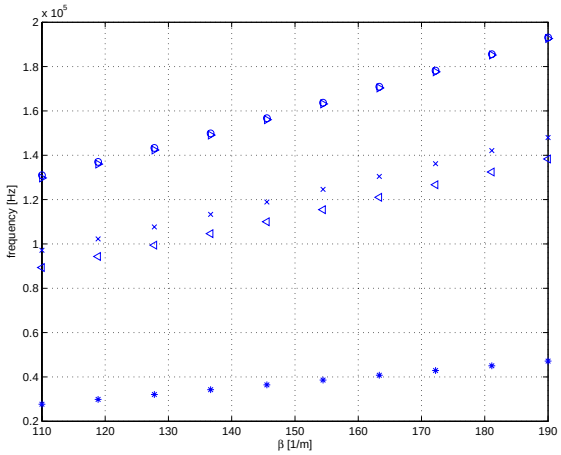

Fig. 9. Plot of the first bands (in frequency) in the β interval: $110-180$ m^{-1} for a structure composed of an A layer (steel) with thickness 0.005 m and a B-layer(water) with thickness 0.001 m.

and also the linear dependence with fluid flow velocity. In the lower plot, the relative change in group velocity due to the fluid flow is shown.

We next consider the case with finite values of β, ω. In Figure 8 a plot of the first bands (in frequency) in the β interval: $110 - 180$ m^{-1} for a structure composed of an A layer (steel) with thickness 0.01 m and a B-layer(water) with thickness 0.001 m. Notice, as expected, that for each β value a discrete set of possible ω solutions exist. In Figure 9, a similar calculation is shown for the case with an A-layer (steel) thickness equal to 0.005 m and a B-layer(water) with thickness 0.001 m.

VI. Conclusions

A discussion of group velocities in structures consisting of alternating layers of piezoelectric cubic crystals (including the case of isotropic crystals) and fluids allowing for a flow in the fluid layers is presented. The thicknesses of each of the solid and fluid layers can be arbitrary. It is found using the Hamiltonian equations that a single equation for the group velocity is obtained at small frequencies even in the presence of a flow. Special consideration is provided for flow-velocity dependencies and sensitivities of the group velocity. In the second part of the paper, special attention is given to the general frequency case of a solid-fluid alternatingly-stacked finite structure and the formation of bandstructures. These results apply to the case of infinite number of layers as well.

References

[1] M.S. Kushwaha, P. Halevi, L. Dobrzynski, and B. Djafari-Rouhani, "Acoustic Band Structure of Periodic Elastic Composites," Phys. Rev. Lett, 71, 2022-2025 (1993).
[2] C.M. Soukoulis, S. Datta, and E.N. Economou, "Propagation of classical waves in random media," 49, 3800-3811 (1994).
[3] M.S. Kushwaha, B. Djaraf-Rouhani, and L. Dobrzynski, "Sound isolation from cubic arrays of air bubbles in water," Phys. Lett. A, 248, 252-256 (1998).
[4] A.A Krokhin, J. Arriaga, and L.N. Gumen, "Speed of sound in periodic elastic composites," Phys. Rev. Lett. 91, 264302-1-4 (2004).
[5] M. Kafesaki, R.S. Penciu, and E.N. Economou, "Air bubbles in water: A strongly mulitple scattering medium for acoustic waves," Phys. Rev. Lett., 84, 6050-6053 (2000).
[6] M. Willatzen and L.C. Lew Yan Voon, "Flow acoustics in periodic structures," Ultrasonics, 43, 756-763 (2005).
[7] M. Deryabin and M. Willatzen, "On acoustic bandgap structure in finite alternating domains,"WSEAS Transactions on Mathematics, 8, 969-977 (2006).
[8] M. Deryabin and M. Willatzen, "Stability investigations in acoustic flows," WSEAS Transactions on Mathematics, 8, 961-968 (2006).
[9] F. Cervera, L. Sanchez, J.V. Sanchez-Perez, R. Martinez-Sala, C. Rubio, F. Meseguer, C. Lopez, D. Caballero, and J. Sanchez-Dehesa, Phys. Rev. Lett. 88, 023902 (2002).
[10] J.V. Sanchez-Perez, D. Caballero, R. Martinez-Sala, C. Rubio, J. Sanchez-Dehesa, F. Meseguer, J. Llinares, and F. Galvez, Phys. Rev. Lett. 80, 5325-5328 (1998).
[11] Gail ter Haar, Phys. Today 54, 29 (2001).
[12] B.A. Auld, "Acoustic Fields and Waves in Solids," Volume I, Second Edition, Krieger Publishing Company (1990).
[13] Whittaker, "A treatise on the analytical dynamics of rigid bodies and systems," Fourth Edition, Cambridge Mathematical Library (1988).

Morten Willatzen, Ph.D., is a Professor and group leader of mathematical modelling, University of Southern Denmark, since 2000. He received the M.Sc. degree in mathematical physics from the University of Aarhus, Denmark in 1989 and the Ph.D. degree in theoretical physics from the Niels Bohr Institute, University of Copenhagen, Denmark in 1993. MW has occupied research positions at the University of Tokyo, Japan, and Max-Planck Institute für Festkörperforschung, Stuttgart, Germany, and Danfoss A/S after his Ph.D. degree. MW's research interests include: solid state physics - in particular - quantum-confined structures and applications to semiconductor laser amplifiers, ultrasonics, flow acoustics, transducer modelling, and modelling of thermo-fluid systems.

Mikhail Vladimirovich Deryabin, Ph.D., dr.scient. is a Professor of mathematical modelling. He received the M.Sc. degree in applied mathematics from Moscow State University, Faculty of Mechanics and Mathematics, Moscow, Russia in 1995, and the Ph.D. (1998) and dr.scient. (2004) degrees in mathematics and physics from the same university. MDs research interests include: mathematical methods in classical mechanics and hydrodynamics (in particular, Hamiltonian mechanics, topological fluid dynamics, Lie groups, symmetries and resonances), and mathematical modelling of physical systems, such as flow acoustics and nano-wires.